

Unexpected Strengthening of the H-Bond Complexes in a Polar Solvent Due to a More Efficient Solvation of the Complex Compared to Isolated Monomers

Vijay Madhav Miriyala,[#] Rabindranath Lo,[#] Petr Bouř, Tau Wu, Dana Nachtigallová,^{*} and Pavel Hobza^{*}



Cite This: *J. Phys. Chem. A* 2022, 126, 7938–7943



Read Online

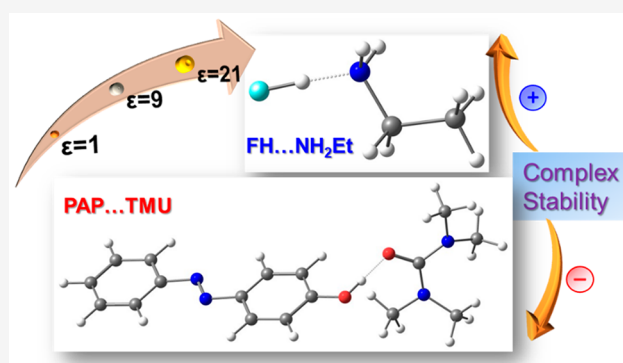
ACCESS |

Metrics & More

Article Recommendations

Supporting Information

ABSTRACT: It is generally assumed that hydrogen-bonded complexes are less stable in solvents than in the gas phase and that their stability decreases with increasing solvent polarity. This assumption is based on the size of the area available to the solvent, which is always smaller in the complex compared to the subsystems, thereby reducing the solvation energy. This reduction prevails over the amplification of the electrostatic hydrogen bond by the polar solvent. In this work, we show, using experimental IR spectroscopy and DFT calculations, that there are hydrogen-bonded complexes whose stability becomes greater with increasing solvent polarity. The explanation for this surprising stabilization is based on the analysis of the charge redistribution in the complex leading to increase of its dipole moment and solvation energy. Constrained DFT calculations have shown a dominant role of charge transfer over polarization effects for dipole moment and solvation energy.



INTRODUCTION

Solvation effects play an essential role in almost all chemical processes, including the formation and stability of supramolecular complexes. It is generally assumed that the stability of covalent complexes is only minimally affected by the character of a solvent. Contrary to these expectations, we found a surprising stabilization of complexes with a dative-covalent bond. In particular, the stability of the complexes with the N → C, N → B, and P → C dative bonds increased in solvents compared to stabilities in the gas phase.^{1–4} The increasing stability was explained by transferring a charge between the electron donor and electron acceptor, leading to an increase of dipole moment in complexes and, consequently, increasing solvation energy of the complexes with respect to energies of their isolated constituents.

There is a general assumption that the stability of hydrogen-bonded complexes decreases in solvents with their increasing polarity.^{5–14} Separated subsystems have larger solvation energies since they are either charged or have substantial dipole moments. In addition, the solvent-accessible surface area (SASA) of a complex is systematically smaller than the sum of SASA of individual subsystems.⁷ Our preliminary results performed on the set of noncovalent complexes¹⁵ indicated that the effect of solvent is more complex.

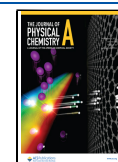
Stabilization of X–H...Y H-bond, where X–H is a proton donor and Y is a proton acceptor, is due to electrostatic interactions between positively charged hydrogen and

negatively charged electron donor Y.^{16,17} These interactions explain the stabilization of the H-bond complexes due to the elongation of the X–H bond, which increases the X–H dipole moment and thus the dipole–dipole interaction between the proton donor and acceptor.¹⁸ The electrostatic interactions are thus responsible for the geometrical, energetic, and vibrational properties of the complex. As discussed by Coulson,¹⁹ it is necessary to include charge transfer (or delocalization effect) in the description of the complex. Although the concept of charge transfer (CT) in hydrogen bonding is somewhat unclear, its contribution to hydrogen bonding has been demonstrated by NBO orbital analyses. These analyses, performed on several H-bond complexes by Reed et al.,²⁰ revealed charge transfer from the lone pair of Y to the X–H σ^* antibonding orbital. The increase in electron density in σ^* antibonding orbital weakens the X–H covalent bond and lowers the X–H stretching frequency. The insufficiency of the description of H-bonding (and other noncovalent interactions) using only electrostatic contributions²¹ and the importance of including contributions describing charge transfer/electron

Received: August 22, 2022

Revised: October 10, 2022

Published: October 20, 2022



delocalization has also been highlighted in recent papers of Murray and Politzer²² and van der Lubbe and Guerra.²³

Despite the ambiguity of the concept of CT in the H-bonding and in view of previous demonstrations of its applicability in the description of H-bonded complexes, we use the relative CT values for the explanation of H-bonded complex stabilities in various solvents. The effect of CT is further discussed based on the results of calculations in which its contribution is eliminated (see below for the constrained DFT calculations). Finally, the correlation/dispersion energy also has a non-negligible contribution to stabilizing H-bonded complexes.¹⁶ The solvent plays a dual role in the resulting stability of the complexes: it modifies the structure of all systems and also CT between electron and proton donors. Besides H-bond strength, modified CT also affects the electrostatic properties of a complex and thus its solvation energy. The overall stability of the complex in a solvent provided by association (equilibrium) constants or binding free energies comprises two contributions, H-bonding modified by solvent and changes in solvation energy. Our goal is to investigate the role of bulk solvents, not the specific interaction of the H-bonded complex with one or more solvent molecules. These so-called cooperative hydrogen bonding effects have been attributed to polarization, not charge transfer, and have been extensively studied in the past.²⁴

In this work, we aim to study in detail, using experimental and computational methods, the effects of solvents on the stability of H-bonded complexes. First, we investigate the origin of the stability of H-bonded complexes in nonpolar and polar solvents. To avoid cooperative effects, only aprotic solvents were considered. Besides spectroscopic characteristics describing H-bonding, we also discuss the binding free energies or association constants. Two H-bonded complexes, 4-(phenylazo)phenol (PAP)⋯tetramethylurea (TMU) and FH⋯ethylamine (EA) (Figure 1), are considered in this

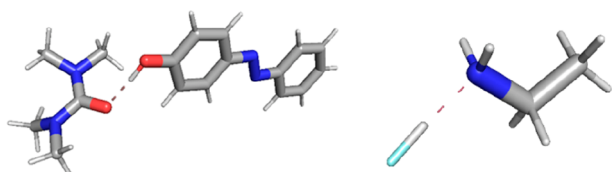


Figure 1. Optimized structures of PAP⋯TMU and FH⋯EA. Color code: C, gray; N, blue; H, white; F, cyan.

study. In the case of the former complex, experimental association constants previously determined with UV/vis absorption titration²⁵ and observed IR frequencies measured in different solvents are supplemented by us with the corresponding calculated values. Agreement between experimental and calculated binding free energies found for this complex justifies using calculated binding free energies for the FH⋯EA complex which cannot be prepared in the required 1:1 stoichiometry.

METHODS

Experimental Section. 4-(Phenylazo)phenol was added to deuterated chloroform (CDCl₃) and tetrachloromethane (CCl₄) in 0.1 M concentration. The compound did not dissolve completely and a milky suspension was obtained. For the complex, tetramethylurea was added to the solution to the same (0.1 M) concentration, which resulted in a transparent

solution. FTIR spectra were recorded on the Biotools ChiralIR spectrometer at 4 cm⁻¹ resolution, at room temperature, in a CaF₂ cell, using a 100 μm spacer. Spectra of pure solvents were subtracted as a baseline.

Calculations. The structures were optimized at the DFT-D level using the PBE0-D3^{26,27} functional with zero damping and def2-TZVPP basis set.²⁸ Using the same level, the Gibbs binding free energies (ΔG_{calc}) at 298 K were evaluated with the ideal gas approximation of the rigid rotor–harmonic oscillator. Effects of solvents were modeled with the COSMO solvation model.²⁹ Solvent environments were characterized by their corresponding dielectric constants ϵ , gas phase ($\epsilon = 1$), *n*-octane ($\epsilon = 1.9$), tetrachloromethane ($\epsilon = 2.2$), toluene ($\epsilon = 2.4$), chloroform ($\epsilon = 4.8$), dibromomethane ($\epsilon = 7.2$), dichloromethane ($\epsilon = 8.9$), and acetone ($\epsilon = 20.7$). The validity of the implicit solvent model was verified using the explicit solvent model. The contribution of solvent to the overall stability was determined by the change of solvation energy (ΔE^{solv}), which corresponds to the difference between the solvation energies of the complex and separated subsystems, respectively. The solvation energy (E^{solv}) of the system in a particular solvent is determined as a difference between the energy of the optimized system in that solvent and the energy of that geometry in the gas phase. A negative value of ΔE^{solv} indicates that the complex is more stabilized by a solvent than the subsystems. Charge transfers were evaluated using the NBO analyses.³⁰ All calculations were performed using Gaussian 16 program package.³¹

Charge transfer based on NBO atomic charges plays an essential role in the complex's characterization in the present paper. Although the whole concept of charge transfer in NBO analyses is not well-defined and its value depends on a computation strategy, we rely on our previous experience gained in the calculations performed on noncovalent complexes from S20, S66, and X40 data sets.¹⁵ In this study, we used the CT values determined by a Řezáč and de la Lande technique³² based on the spatial definition of molecular fragments using the superimposed electron density of isolated noninteracting fragments as a reference state. These benchmark CT values were closely correlated with the CT values based on NBO charges, justifying the use of the latter approach in the present paper.

Dipole moments of FH⋯NH₂Et and PAP⋯TMU complexes were calculated with and without CT. The latter dipole moment was obtained via constrained DFT calculations in which intermolecular CT is eliminated. The constrained DFT (cDFT) calculations³³ were performed at PBE0-D3/def2-TZVPP level using NWCHEM version 7.0.2.³⁴ cDFT takes account of the effects of polarization and orbital relaxation using many-body wave functions describing localized charges. Such wave functions are achieved within DFT by revising the Kohn–Sham equations comprising a spatially dependent potential, whose strength is varied self-consistently to fulfill the constraint of the desired number of electrons localized on a given fragment.³³

Explicit Solvent Models. We simulated the molecular dynamics trajectories using ORCA 4.2.1 code³⁵ and visualized them using VMD 1.9.2 visualization software.³⁶ All the simulations were performed at the PBE0-D3BJ/6-31G* level of theory. The simulations were performed up to 20 ps time scale. The step size was set to 1 fs, a Berendsen thermostat³⁷ with a time constant of 20 fs was employed to control the temperatures. The temperature for all the simulations was set

at 300 K. Selected frames from the trajectories for both the solvents were then optimized at PBE0-D3/6-31G* level.

RESULTS AND DISCUSSION

The IR spectra of PAP and the PAP...TMU complex in CDCl₃ and CCl₄ are shown in Figure 2. The spectra show a significant

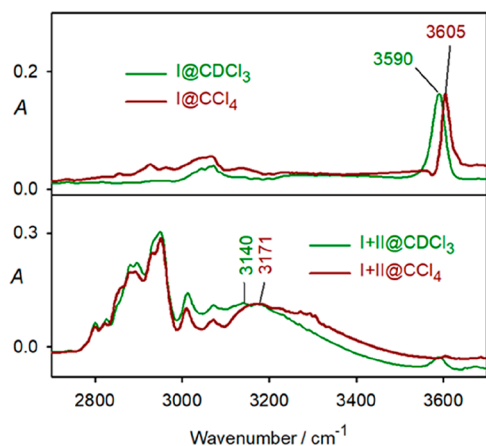


Figure 2. IR spectra comprising the O–H stretching bands (frequencies are indicated) of PAP (I) and PAP in the PAP...TMU (I + II) complex in CDCl₃ and CCl₄. Due to differences in concentration, the CCl₄ intensities were normalized to the CDCl₃ intensities.

red shift of OH stretching frequency ($\Delta\nu$) in the PAP...TMU complex compared to isolated PAP. The increased values of the red shift, 434 cm⁻¹ in CCl₄ ($\epsilon = 2.2$) and 450 cm⁻¹ in CDCl₃ ($\epsilon = 4.8$), indicate a weakening of the intramolecular O–H bond, which increases with the increasing polarity of the solvent. Table 1 summarizes the optimized O–H bond lengths and calculated O–H stretching frequencies in the gas phase and various solvents. In addition, the frequency shifts due to the complex formation are also presented. A comparison of the calculated and observed frequency shifts shows a sizable overestimation of calculated values. However, the observed trend is well reproduced in calculations, justifying their use for discussion in our selection of solvents.

In the gas phase, the formation of the PAP...TMU complex with O–H...O motif lengthens the intramolecular O–H bond by 0.024 Å, further increased by up to 0.038 Å when switching to more polar solvents ($\epsilon > 7$, Table 1). The complexation is accompanied by the red shift of the OH stretching frequency, whose values gradually increase with increasing solvent polarity (see Table 1).

Simultaneously, the intermolecular H...O bond decreases from 1.700 to 1.597 Å, with ϵ values ranging from 1 (gas phase) to 20.7 (acetone). The corresponding stretching frequency shifts from 163 to 185 cm⁻¹. These findings indicate an enhancement of H-bonding in the complex in more polarized solvents.

Despite the above observations, the association constants determined by UV/vis absorption or ¹H NMR show a decrease of more than 3 orders of magnitude with increasing solvent polarity²⁵ (K_a ($\epsilon = 1.9$) = 2400 M⁻¹, K_a ($\epsilon = 2.4$) = 230 M⁻¹, K_a ($\epsilon = 4.8$) = 52 M⁻¹ and K_a ($\epsilon = 20.7$) = 2 M⁻¹).

Table 1 and Table S1 also report the results of calculations of interaction energies (ΔE), binding free energies (ΔG_{calc}), and solvation energies (ΔE^{solv}) obtained for various solvents. A

good agreement between the experimental binding free energies (ΔG_{exp}), determined from the reported association constants, with ΔG_{calc} values, shown in Figure 3, justifies their use to discuss the stability of the FH...NH₂Et complex in solvents (see below) for which the experimental studies are nonfeasible.

The values of the interaction energies of the complex decrease with increasing solvent polarity, from $\Delta E = -14.2$ kcal/mol in the gas phase ($\epsilon = 1.0$) to $\Delta E = -9.8$ kcal/mol in acetone ($\epsilon = 20.7$) in the COSMO model. The other solvation models also follow the same trend (Table S2). The values of ΔG_{calc} show that while the system is stable at room temperature in the gas phase, it becomes unstable in more polar solvents. The trend in solvation energies shows similar behavior, i.e., as the destabilization of the complex increases, the ΔE^{solv} decreases (see Table 1 and Figure S1). These changes correlate with a decrease in the SASA of the complex compared to the isolated subsystems, specifically by 25.0, 24.5, 22.7, 22.2, 22.0, and 21.9 Å² for solvents with increasing dielectric constant, i.e., in the range of 1 for the gas phase to 20.7 in acetone (Table S3). The other characteristics listed in Table 1, the CT in the complex and the values of intermolecular $r(\text{O}\cdots\text{H})$ distances, explain these changes in solvation energies and the resulting destabilization of the complex as follows: With increasing hydrogen bond strength in polar solvents, demonstrated by the elongation of the intramolecular O–H bond and shortening of the intermolecular O...H bond, the charge transfer in the complex increases (cf. the CT values in Table 1 for optimized geometries (CT) and those in the gas phase (CT(G))). At the same time, SASA decreases (for the correlation between CT and ΔE^{solv} ; see Supporting Information, Figure S2) with the lengthening of the intermolecular O...H bond and so does the solvent stabilization of the complex as compared to results for the isolated subsystems. As a result, the stability of the complex decreases with increasing solvent polarity.

The intramolecular F–H and intermolecular FH...N hydrogen bonds in the FH...NH₂Et complex (see Figure 1 and Table 1) show the same trends as in the case of the PAP...TMU complex, but the solvent effect is much greater. The F–H bond lengthens by 0.047 and 0.129 Å in the gas phase and acetone, respectively, and the FH...N bond shortens by 0.233 Å in the acetone solvent compared to the gas phase. The formation of the H-bond is reflected by a very large red shift of the F–H stretching frequency (1000 cm⁻¹) which further increases in acetone solvent (2402 cm⁻¹). The strengthening of the H-bond is also reflected by the large blue shift of intermolecular H...N stretching frequency (by 47 cm⁻¹) in acetone solvent. The interaction energies of both complexes are comparable in the gas phase. Unlike the PAP...TMU complex, the interaction in FH...NH₂Et strengthens with the increasing polarity of the solvent (cf. ΔE values of -15.8 kcal/mol in the gas phase to -17.4 kcal/mol in acetone and ΔG_{calc} of -5.9 kcal/mol in the gas phase and -7.6 kcal/mol in acetone, respectively, Table 1 and Table S1). Although the SASA of the FH...NH₂Et decreases compared to the isolated subsystems, as in the case of the PAP...TMU, the changes in the solvation energies demonstrate a larger contribution to the overall FH...NH₂Et stability in a solvent. Thus, in the case of the FH...NH₂Et, the polarity of the solvent affects the stability of the hydrogen-bonded complex in a way not previously reported: the stability of the complex becomes greater with increasing solvent polarity. The explanation for this surprising

Table 1. Interaction Energies (ΔE), Free Energies (ΔG_{calc}), and Solvation Energies (ΔE^{solv}) in kcal/mol, Charge Transfer in Corresponding Medium (CT) and Charge Transfer of Gas-Phase Geometry in Corresponding Medium (CT(G)) in electrons, Frequency of the Intramolecular O–H and F–H Bonds in the Monomer ($\nu_{\text{str}}(\text{O–H})$, $\nu_{\text{str}}(\text{F–H})$), Difference in Frequency of the Intramolecular O–H and F–H Bonds in the Monomer and Complex ($\Delta\nu$), Frequency of the Intermolecular H \cdots O Bond ($\nu(\text{H}\cdots\text{O})$) and Intermolecular H \cdots N Bond ($\nu(\text{H}\cdots\text{N})$) in cm^{-1} , Intramolecular O–H and F–H Bond Lengths for Monomer ($r(\text{O–H})$, $r(\text{F–H})$), Difference in Distance of the Intramolecular O–H and F–H Bonds in Monomer and Complex (Δr), and Intermolecular $r(\text{H}\cdots\text{O})$ and $r(\text{H}\cdots\text{N})$ bond lengths in \AA ^a

PAP \cdots TMU	ΔE	ΔG_{calc}	ΔE^{solv}	CT	CT(G)	$\nu_{\text{str}}(\text{O–H})/\Delta\nu$		$\nu(\text{H}\cdots\text{O})$	$r(\text{O–H})/\Delta r$	$r(\text{H}\cdots\text{O})$
						calc	exp			
gas	–14.2	–2.2		–0.048	–0.048	3877/488		163	0.959/0.024	1.700
<i>n</i> -octane ($\epsilon = 1.9$)	–12.2	–0.8	1.9	–0.058	–0.051	3857/633		176	0.961/0.030	1.646
CCl_4 ($\epsilon = 2.2$)	–11.9	–0.7	2.2	–0.060	–0.051	3854/659	3605/434	177	0.961/0.031	1.638
toluene ($\epsilon = 2.4$)	–11.8	–0.5	2.4	–0.061	–0.051	3852/661		178	0.961/0.032	1.637
CDCl_3 ($\epsilon = 4.8$)	–10.7	0.0	3.4	–0.066	–0.053	3840/727	3590/449	182	0.962/0.034	1.616
dibromomethane ($\epsilon = 7.2$)	–10.3	1.1	3.8	–0.069	–0.053	3836/756		183	0.962/0.036	1.607
dichloromethane ($\epsilon = 8.9$)	–10.1	1.3	3.9	–0.070	–0.053	3834/765		184	0.963/0.038	1.604
acetone ($\epsilon = 20.7$)	–9.8	1.9	4.0	–0.072	–0.054	3829/785		185	0.963/0.037	1.597
FH \cdots NH ₂ Et	ΔE	ΔG_{calc}	ΔE^{solv}	CT	CT(G)	$\nu_{\text{str}}(\text{F–H})/\Delta\nu$		$\nu(\text{H}\cdots\text{N})$	$r(\text{F–H})/\Delta r$	$r(\text{H}\cdots\text{N})$
						calc	exp			
gas	–15.8	–5.9		–0.084	–0.084	4155/1000		255	0.918/0.047	1.623
<i>n</i> -octane ($\epsilon = 1.9$)	–16.2	–6.2	–0.6	–0.117	–0.093	4160/140			0.918/0.008	
CCl_4 ($\epsilon = 2.2$)	–16.3	–6.3	–0.9	–0.124	–0.094	4112/1418		274	0.920/0.068	1.537
						4110/109			0.921/0.006	
toluene ($\epsilon = 2.4$)	–16.3	–6.3	–1.0	–0.126	–0.095	4105/1501		277	0.921/0.072	1.522
						4105/			0.921/	
chloroform ($\epsilon = 4.8$)	–16.8	–6.8	–2.2	–0.155	–0.100	4102/1538		279	0.921/0.074	1.516
						4101/105			0.921/0.006	
dibromomethane ($\epsilon = 7.2$)	–17.0	–7.1	–2.9	–0.169	–0.102	4078/1915		290	0.922/0.097	1.458
						4075/91			0.923/0.005	
dichloromethane ($\epsilon = 8.9$)	–17.1	–7.3	–3.2	–0.175	–0.102	4069/2100		295	0.923/0.108	1.432
						4065/87			0.924/0.004	
acetone ($\epsilon = 20.7$)	–17.4	–7.6	–4.2	–0.192	–0.104	4065/2178		297	0.923/0.113	1.421
						4062/84			0.924/0.004	
						4057/2402		302	0.924/0.129	1.390
						4052/78			0.924/0.004	

^aThe calculated values using constrained DFT method are given in italics. The dielectric constant (ϵ) of each solvent is given in parentheses.

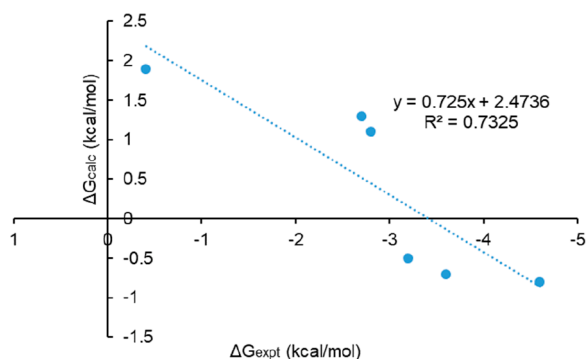


Figure 3. Correlation between ΔG_{exp} (calculated from the reported²⁵ association constants) and ΔG_{calc} for PAP \cdots TMU. The values are in kcal/mol.

behavior lies in the dipole moment and CT values (Table 1), which are significantly larger than those of PAP \cdots TMU already in the gas and increase much more significantly in solvents. Table 1 also displays the values of F–H distances and stretching frequencies calculated using constrained DFT,

showing that when the CT is suppressed, the changes upon complexation are about an order of magnitude smaller in all cases. In addition, the calculated dipole moment values obtained through nonconstrained and constrained DFT calculations indicate that CT has a major contribution to the dipole moment. Specifically for PAP \cdots TMU, it decreases from 3.1 to 1.9 D (40%) when CT contributions are switched off. This reduction is even higher for FH \cdots NH₂Et: from 4.8 to 2.4 D, i.e., by 50%. The comparison of the solvation energies obtained for the nonconstrained and constrained DFT calculations of FH \cdots NH₂Et in the various solvents is even more illustrative: In the first calculations, solvation stabilizes the complex, and this effect increases by 3.8 kcal/mol in the transition from *n*-octane to acetone. Turning off the CT contributions causes the solvent to destabilize the complex by 3.3 kcal/mol more in acetone than in *n*-octane. Similarly for the PAP \cdots TMU complex, the transition from *n*-octane to acetone solvation destabilizes the complex (by 2.2 kcal/mol), and this destabilization increases to 4.0 kcal/mol when CT is neglected (constrained DFT).

The calculations modeling the solvent control were based on a continuous solvent model, where the solvent is characterized

by its dielectric constant. A more reliable explicit solvent model provided similar results, as shown by the results obtained for the implicit model and the results of molecular dynamics (MD) simulations FH \cdots NH₃ complex (Figure S3). The intermolecular CT -0.072 e predicted in the gas phase increased to -0.116 and -0.154 e in CS₂ and CCl₂H₂, respectively, using implicit solvent calculations. MD simulations, performed in vacuo and embedded in a cluster of 20 molecules of CS₂ and 20 molecules of CCl₂H₂ provided very similar values of -0.090 and -0.144 e. Similarly, the intermolecular N \cdots H distance decreased from 1.666 Å (gas phase) to 1.549 Å (CS₂) and 1.470 Å (CCl₂H₂), respectively, in the calculations with implicit solvent. By comparison, the explicit model provided qualitatively comparable values of 1.695, 1.530, and 1.230 Å, respectively.

CONCLUSIONS

The increasing polarity of the solvent results in the well-known enhancement of intermolecular bond strength in hydrogen-bonded complexes, demonstrated in the IR spectra by the increased red shift of OH stretching and blue shift of intermolecular H \cdots Y stretching frequency. Simultaneously, with the strengthening of the hydrogen bond, the surface area reachable by the solvent decreases, resulting in changes in the stability of the complex. In this work, we have shown that in addition to the expected destabilization in solvents, a surprising stabilization can be observed even though the SASA decreases.

This surprising observation can be explained based on the charge transferred during complex formation. This magnitude always increases as the solvent becomes more polar. In the case of PAP \cdots TMU, in the formation of which charge transfer occurs only marginally, the destabilization due to the lower SASA value prevails. In the case of FH \cdots NH₂Et, the charge transfer due to complexation is already significant in the gas phase and further increases in the solvent. This leads to a relatively large dipole moment in the complex, which results in its stabilization in a solvent. Constrained DFT calculations have shown that the significant increase in the solvation energy of the complex in polar solvents is due to CT and not polarization. Our results indicate that there exists some borderline (estimated in the present study ranging approximately -0.05 to -0.08 e, based on DFT-D3/PBE0-D3/def2-TZVPP NBO charges) at which the solvent stabilizes/destabilizes a hydrogen-bonded complex, providing a 2-fold role of the solvent. The present study provides an additional piece of information on the complex role of the solvent on the stability of covalent/dative and noncovalent systems.

ASSOCIATED CONTENT

Supporting Information

The Supporting Information is available free of charge at <https://pubs.acs.org/doi/10.1021/acs.jpca.2c05992>.

Correlation between calculated ΔG_{expt} and ΔE_{solv} and between calculated ΔE_{solv} and CT and gemoetry diagram (Figures S1–S3), thermodynamic properties and surface areas (Tables S1–S3), and Cartesian coordinates of the optimized structures (PDF)

AUTHOR INFORMATION

Corresponding Authors

Dana Nachtigallová – Institute of Organic Chemistry and Biochemistry, Czech Academy of Sciences, 16000 Prague, Czech Republic; IT4Innovations, VSB-Technical University of Ostrava, 70800 Ostrava, Poruba, Czech Republic; orcid.org/0000-0002-9588-8625; Email: dana.nachtigallova@uochb.cas.cz

Pavel Hobza – Institute of Organic Chemistry and Biochemistry, Czech Academy of Sciences, 16000 Prague, Czech Republic; IT4Innovations, VSB-Technical University of Ostrava, 70800 Ostrava, Poruba, Czech Republic; orcid.org/0000-0001-5292-6719; Email: pavel.hobza@uochb.cas.cz

Authors

Vijay Madhav Miriyala – Institute of Organic Chemistry and Biochemistry, Czech Academy of Sciences, 16000 Prague, Czech Republic; Regional Centre of Advanced Technologies and Materials, Czech Advanced Technology and Research Institute, Palacký University, 77900 Olomouc, Czech Republic; orcid.org/0000-0003-3926-9691

Rabindranath Lo – Institute of Organic Chemistry and Biochemistry, Czech Academy of Sciences, 16000 Prague, Czech Republic; Regional Centre of Advanced Technologies and Materials, Czech Advanced Technology and Research Institute, Palacký University, 77900 Olomouc, Czech Republic; orcid.org/0000-0002-4436-3618

Petr Bouř – Institute of Organic Chemistry and Biochemistry, Czech Academy of Sciences, 16000 Prague, Czech Republic

Tau Wu – Institute of Organic Chemistry and Biochemistry, Czech Academy of Sciences, 16000 Prague, Czech Republic

Complete contact information is available at: <https://pubs.acs.org/10.1021/acs.jpca.2c05992>

Author Contributions

[#]V.M.M. and R.L. can be considered as first authors.

Notes

The authors declare no competing financial interest.

ACKNOWLEDGMENTS

This work was supported by the Czech Science Foundation, projects 19-27454X (to P.H. and D.N.) and 20-10144S (to P.B.).

REFERENCES

- (1) Lamanec, M.; Lo, R.; Nachtigallová, D.; Bakandritsos, A.; Mohammadi, E.; Dračinský, M.; Zbořil, R.; Hobza, P.; Wang, W. The Existence of a N \rightarrow C Dative Bond in the C₆₀–Piperidine Complex. *Angew. Chem., Int. Ed.* **2021**, *60*, 1942–1950.
- (2) Lo, R.; Manna, D.; Lamanec, M.; Wang, W.; Bakandritsos, A.; Dračinský, M.; Zbořil, R.; Nachtigallová, D.; Hobza, P. Addition Reaction between Piperidine and C₆₀ to Form 1,4-Disubstituted C₆₀ Proceeds through van der Waals and Dative Bond Complexes: Theoretical and Experimental Study. *J. Am. Chem. Soc.* **2021**, *143*, 10930–10939.
- (3) Lo, R.; Manna, D.; Lamanec, M.; Dračinský, M.; Bouř, P.; Wu, T.; Bastien, G.; Kaleta, J.; Miriyala, V. M.; Špirko, V.; Mašínová, A.; Nachtigallová, D.; Hobza, P. The stability of covalent dative bond significantly increases with increasing solvent polarity. *Nat. Commun.* **2022**, *13* (2107), 2107.
- (4) Lo, R.; Lamanec, M.; Wang, W.; Manna, D.; Bakandritsos, A.; Dračinský, M.; Zbořil, R.; Nachtigallová, D.; Hobza, P. Structure-

directed formation of the dative/covalent bonds in complexes with C₇₀-piperidine. *Phys. Chem. Chem. Phys.* **2021**, *23*, 4365–4375.

(5) Driver, M. D.; Williamson, M. J.; Cook, J. L.; Hunter, C. A. Functional group interaction profiles: a general treatment of solvent effects on non-covalent interactions. *Chem. Sci.* **2020**, *11*, 4456–4466.

(6) Cook, J. L.; Hunter, C. A.; Low, C. M. R.; Perez-Velasco, A.; Vinter, J. G. Solvent Effects on Hydrogen Bonding. *Angew. Chem., Int. Ed.* **2007**, *46*, 3706–3709.

(7) Aquino, A. J. A.; Tunega, D.; Haberhauer, G.; Gerzabek, M. H.; Lischka, H. Solvent Effects on Hydrogen Bonds A Theoretical Study. *J. Phys. Chem. A* **2002**, *106*, 1862–1871.

(8) Robertson, C. C.; Wright, J. S.; Carrington, E. J.; Perutz, R. N.; Hunter, C. A.; Brammer, L. Hydrogen bonding vs. halogen bonding: the solvent decides. *Chem. Sci.* **2017**, *8*, 5392–5398.

(9) Zuo, J.; Zhao, B.; Guo, H.; Xie, D. A global coupled cluster potential energy surface for HCl + OH \leftrightarrow Cl + H₂O. *Phys. Chem. Chem. Phys.* **2017**, *19*, 9770–9777.

(10) Wang, J.; Shao, L.; Yan, P.; Liu, C.; Liu, X.; Zhang, X. M. Are solvent effects important for intramolecular C–H...O– hydrogen bonding interactions? *J. Phys. Org. Chem.* **2019**, *32*, e3912.

(11) Hunter, C. A. Quantifying Intermolecular Interactions: Guidelines for the Molecular Recognition Toolbox. *Angew. Chem., Int. Ed.* **2004**, *43*, 5310–5324.

(12) Cabot, R.; Hunter, C. A. Non-covalent interactions between iodo-perfluorocarbons and hydrogen bond acceptors. *Chem. Commun.* **2009**, 2005–2007.

(13) Meredith, N. Y.; Borsley, S.; Smolyar, I. V.; Nichol, G. S.; Baker, C. M.; Ling, K. B.; Cockroft, S. L. Dissecting Solvent Effects on Hydrogen Bonding. *Angew. Chem., Int. Ed.* **2022**, *61*, e202206604.

(14) Burns, R. J.; Mati, I. K.; Muchowska, K. B.; Adam, C.; Cockroft, S. L. Quantifying Through-Space Substituent Effects. *Angew. Chem., Int. Ed.* **2020**, *59*, 16717–16724.

(15) Lo, R.; Mašínová, A.; Lamanec, M.; Nachtigallová, D.; Hobza, P. The unusual stability of H-bonded complexes in solvent caused by greater solvation energy of complex compared to those of isolated fragments. *J. Comput. Chem.* **2022**, DOI: 10.1002/jcc.26928.

(16) Kolář, M. H.; Hobza, P. Computer Modeling of Halogen Bonds and Other sigma-Hole Interactions. *Chem. Rev.* **2016**, *116*, 5155–5187.

(17) Hobza, P.; Havlas, Z. Blue-Shifting Hydrogen Bonds. *Chem. Rev.* **2000**, *100*, 4253–4264.

(18) Hobza, P.; Muller-Dethlefs, K. *Non-Covalent Interactions: Theory and Experiment*; Royal Society of Chemistry: Cambridge, 2009; pp 134–154.

(19) Coulson, C. A. The hydrogen bond—a review of the present position. *Res. Appl. Ind.* **1957**, *149*, 10.

(20) Reed, A. E.; Weinhold, F.; Curtiss, L. A.; Pochatko, D. J. Natural bond orbital analysis of molecular interactions: Theoretical studies of binary complexes of HF, H₂O, NH₃, N₂, O₂, F₂, CO, and CO₂ with HF, H₂O and NH₃. *J. Chem. Phys.* **1986**, *84*, 5687.

(21) Hermansson, K. Blue-Shifting Hydrogen Bonds. *J. Phys. Chem. A* **2002**, *106*, 4695–4702.

(22) Murray, J. S.; Politzer, P. Interaction and Polarization Energy Relationships in σ -Hole and π -Hole Bonding. *Crystals* **2020**, *10* (2), 76.

(23) van der Lubbe, S. C. C.; Guerra, C. F. The Nature of Hydrogen Bonds: A Delineation of the Role of Different Energy Components on Hydrogen Bond Strengths and Lengths. *Chem.—Asian J.* **2019**, *14*, 2760–2769.

(24) Mahadevi, A. S.; Sastry, G. N. Cooperativity in Noncovalent Interactions. *Chem. Rev.* **2016**, *116*, 2775–2825.

(25) Robertson, C. C.; Perutz, R. N.; Brammer, L.; Hunter, C. A. A solvent-resistant halogen bond. *Chem. Sci.* **2014**, *5*, 4179–4183.

(26) Adamo, C.; Barone, V. Toward reliable density functional methods without adjustable parameters: The PBE0 model. *J. Chem. Phys.* **1999**, *110*, 6158–6170.

(27) Grimme, S.; Antony, J.; Ehrlich, S.; Krieg, H. A consistent and accurate ab initio parametrization of density functional dispersion

correction (DFT-D) for the 94 elements H–Pu. *J. Chem. Phys.* **2010**, *132*, 154104–154119.

(28) Weigend, F. Hartree–Fock exchange fitting basis sets for H to Rn. *J. Comput. Chem.* **2008**, *29*, 167–175.

(29) Klamt, A.; Schürmann, G. COSMO: a new approach to dielectric screening in solvents with explicit expressions for the screening energy and its gradient. *J. Chem. Soc., Perkin Trans.* **1993**, *2*, 799–805.

(30) Reed, A. E.; Curtiss, L. A.; Weinhold, F. Intermolecular interactions from a natural bond orbital, donor-acceptor viewpoint. *Chem. Rev.* **1988**, *88*, 899–926.

(31) Frisch, M. J.; Trucks, G. W.; Schlegel, H. B.; Scuseria, G. E.; Robb, M. A.; Cheeseman, J. R.; Scalmani, G.; Barone, V.; Petersson, G. A.; Nakatsuji, H.; et al. *Gaussian 16*, Revision A.03; Gaussian, Inc.: Wallingford, CT, 2016.

(32) Rezac, J.; de la Lande, A. On the role of charge transfer in halogen bonding. *Phys. Chem. Chem. Phys.* **2017**, *19*, 791–803.

(33) Kaduk, B.; Kowalczyk, T.; Van Voorhis, T. Constrained Density Functional Theory. *Chem. Rev.* **2012**, *112*, 321. and references therein.

(34) Apra, E.; Bylaska, E. J.; De Jong, W. A.; Govind, N.; Kowalski, K.; Straatsma, T. P.; Valiev, M.; van Dam, H.; Alexeev, Y.; Anchell, J.; et al. NWChem: Past, present, and future. *J. Chem. Phys.* **2020**, *152*, 184102.

(35) Neese, F. The ORCA program system. *Wiley Interdiscip. Rev.: Comput. Mol. Sci.* **2012**, *2*, 73–78.

(36) Humphrey, W.; Dalke, A.; Schulten, K. VMD: Visual molecular dynamics. *J. Mol. Graph.* **1996**, *14*, 33.

(37) Berendsen, H. J. C.; Postma, J. P. M.; van Gunsteren, W. F.; DiNola, A.; Haak, J. R. Molecular dynamics with coupling to an external bath. *J. Chem. Phys.* **1984**, *81*, 3684.

Recommended by ACS

Intermolecular Interactions Involving Heavy Alkenes H₂Si=TH₂ (T = C, Si, Ge, Sn, Pb) with H₂O and HCl: Tetrel Bond and Hydrogen Bond

Yishan Chen and Fan Wang

NOVEMBER 12, 2020
ACS OMEGA

READ 

Molecular Electrostatic Potential Reorganization Theory to Describe Positive Cooperativity in Noncovalent Trimer Complexes

Padinjare Veetil Bijina and Cherumuttathu H. Suresh

FEBRUARY 18, 2020
THE JOURNAL OF PHYSICAL CHEMISTRY A

READ 

Modeling of Ribbon and Oblique Structures of Benzene-1,3,5-triyl-tribenzoic Acid

Andrius Ibenskas and Evaldas E. Tornau

JULY 29, 2020
THE JOURNAL OF PHYSICAL CHEMISTRY C

READ 

Encapsulation of Hydrogen Molecules in C₅₀ Fullerene: An *ab Initio* Study of Structural, Energetic, and Electronic Properties of H₂@C₅₀ and 2H₂@C₅₀ Complexes

Alireza Zeinalinezhad and Riadh Sahnoun

MAY 22, 2020
ACS OMEGA

READ 

Get More Suggestions >